





# Molecular mechanisms of heparin-induced modulation of human interleukin 12 bioactivity

Received for publication, October 9, 2018, and in revised form, January 18, 2019. Published, Papers in Press, January 22, 2019, DOI 10.1074/jbc.RA118.006193

Khue G. Nguyen<sup>‡§</sup>, Francis B. Gillam<sup>§</sup>, Jared J. Hopkins<sup>§</sup>, Srinivas Jayanthi<sup>¶</sup>, Ravi Kumar Gundampati<sup>¶</sup>, Guowei Su<sup>||</sup>, Jenifer Bear<sup>\*\*</sup>, Guy R. Pilkington<sup>\*\*1</sup>, Rashmi Jalah<sup>\*\*2</sup>, Barbara K. Felber<sup>\*\*</sup>, Jian Liu<sup>||</sup>,  Suresh Kumar Thallapuranam<sup>¶</sup>, and  David A. Zaharoff<sup>‡§3</sup>

From the <sup>‡</sup>Department of Microbiology and Immunology, University of North Carolina at Chapel Hill, Chapel Hill, North Carolina 27599, the <sup>§</sup>Joint Department of Biomedical Engineering, University of North Carolina at Chapel Hill and North Carolina State University, Raleigh, North Carolina 27695, the <sup>¶</sup>Department of Chemistry and Biochemistry, University of Arkansas, Fayetteville, Arkansas 72701, the <sup>||</sup>Division of Chemical Biology and Chemistry, Eshelman School of Pharmacy, University of North Carolina at Chapel Hill, Chapel Hill, North Carolina 27599, and the <sup>\*\*</sup>Human Retrovirus Pathogenesis Section, Vaccine Branch, NCI-Frederick, National Institutes of Health, Frederick, Maryland 21702

Edited by George M. Carman

Human interleukin-12 (hIL-12) is a heparin-binding cytokine whose activity was previously shown to be enhanced by heparin and other sulfated glycosaminoglycans. The current study investigated the mechanisms by which heparin increases hIL-12 activity. Using multiple human cell types, including natural killer cells, an IL-12 indicator cell line, and primary peripheral blood mononuclear and T cells, along with bioactivity, flow cytometry, and isothermal titration calorimetry assays, we found that heparin-dependent modulation of hIL-12 function correlates with several of heparin's biophysical characteristics, including chain length, sulfation level, and concentration. Specifically, only heparin molecules longer than eight saccharide units enhanced hIL-12 activity. Furthermore, heparin molecules with three sulfate groups per disaccharide unit outperformed heparin molecules with one or two sulfate groups per disaccharide unit in terms of enhanced hIL-12 binding and activity. Heparin also significantly reduced the EC<sub>50</sub> value of hIL-12 by up to 11.8-fold, depending on the responding cell type. Cytokine-profiling analyses revealed that heparin affected the level, but not the type, of cytokines produced by lymphocytes in response to hIL-12. Interestingly, although murine IL-12 also binds heparin, heparin did not enhance its activity. Using the gathered data, we propose a model of hIL-12 stabilization in which heparin serves as a co-receptor enhancing the interaction between heterodimeric hIL-12 and its receptor subunits. The results of this study provide a foundation for further investigation of heparin's interactions with IL-12 family cytokines and for the use of heparin as an immunomodulatory agent.

Sulfated GAGs,<sup>4</sup> such as heparin and heparan sulfate, interact with and modulate the activities of numerous proteins (1). Although it is well known that heparin and heparan sulfate enhance the activities of growth factors, such as basic fibroblast growth factor (2–4), their effects on cytokines, particularly interleukins, are highly variable and often inhibitory. For example, heparin was shown to bind strongly to human interleukin-2 but has no effect on its bioactivity (5). Interleukin-3–induced proliferation of FDCP-1 cells is inhibited at high heparin concentrations (6). The complex of heparin and interleukin-7 protects this cytokine from proteolytic degradation; however, the growth of interleukin-7–dependent pre-B cells is suppressed by heparin (7). Also, heparin prevents interleukin-10–induced expression of CD16 and CD64 on monocytes/macrophages (8).

IL-12 is a 70-kDa heterodimeric cytokine composed of the p35 and p40 subunits. Although co-expression of both subunits in the same cell is essential to form the biologically active heterodimer (9–11), production of each of the subunits is independently regulated (12). The p40 subunit plays a critical role in enhancing the stability, intracellular trafficking, and export of the p35 subunit (13). These findings were applied for the generation of greatly improved IL-12 DNA plasmids expressing the two subunits in optimal configuration allowing efficient production of human, macaque, and mouse IL-12 p70 cytokines (13).

IL-12, a central regulator of human immunity, has been shown by our group and others to be a heparin-binding protein (14–16). Our previous work identified two heparin-binding domains located on the p40 subunit of hIL-12 (15). These sites were exploited in the single-step purification of tag-less hIL-12 (15). Recently, we demonstrated that heparin binds hIL-12 with low micromolar affinity and increases its activity by severalfold (17). Remarkably, heparin was found to recover hIL-12 signaling in a natural killer cell line, NK-92MI, in which both IL-12

This work was supported by National Institutes of Health Grant from NCI, the Arkansas Biosciences Institute, and by the Intramural Research Program of the NCI, National Institutes of Health (to B. K. F.). The authors declare that they have no conflicts of interest with the contents of this article. The content is solely the responsibility of the authors and does not necessarily represent the official views of the National Institutes of Health.

This article contains Figs. S1–S4.

<sup>1</sup> Present address: ImQuest BioSciences, Frederick, MD 21704.

<sup>2</sup> Present address: GlaxoSmithKline (GSK) Vaccines, Rockville, MD 20850.

<sup>3</sup> To whom correspondence should be addressed: Joint Department of Biomedical Engineering, University of North Carolina at Chapel Hill and North Carolina State University, Raleigh, North Carolina 27695. Tel.: 919-515-6757; E-mail: dazaharo@ncsu.edu.

<sup>4</sup> The abbreviations used are: IL-12, interleukin 12; h, human; m, mouse; GAG, glycosaminoglycan; IFN- $\gamma$ , interferon  $\gamma$ ; LMWH, low-molecular-weight heparin; SEAP, secreted embryonic alkaline phosphatase; ANOVA, analysis of variance; FBS, fetal bovine serum; PBMC, peripheral blood mononuclear cell; HS, heparan sulfate; ITC, isothermal titration calorimetry; ECD, extracellular domain; PDB, Protein Data Bank.

receptor subunits, IL-12R $\beta$ 1 and IL-12R $\beta$ 2, had been functionally deleted via CRISPR/Cas9 genomic editing (17). Ongoing follow-up studies have demonstrated that the genomic editing process likely resulted in expression of mutated receptor subunits that could not bind hIL-12 sufficiently to trigger signaling.<sup>5</sup> However, hIL-12 binding and signaling was at least partially restored in the presence of heparin.

In circulation, IL-12 induces profound systemic inflammation (18). It has been posited, therefore, that binding to sulfated GAGs present in extracellular matrix keeps IL-12 localized to a site of injury or infection and prevents its systemic dissemination. In addition to this localization effect, our recent studies indicated that sulfated GAGs, including heparin, increased IL-12 concentrations at the cell surface (17). Although this is one possible mechanism to increase IL-12 signaling, a more complete picture of how heparin influences IL-12 function is needed.

In this study, because heparin is a polydisperse, heterogeneous polysaccharide, we began by exploring the effects of heparin's biophysical characteristics on IL-12 function to make inferences about heparin's mechanisms of action. Specifically, because chain length, sulfation level, and concentration have been shown to influence heparin's ability to modulate growth factor activity (8, 19–22), we investigated the effects of these characteristics on IL-12 binding and bioactivity. For robustness, bioactivity studies were performed in four different cell types: an NK cell line (NK-92MI), an IL-12 indicator cell line (HEK-Blue<sup>TM</sup> IL-12), as well as PBMCs and T cells from healthy donors. Similar bioactivity experiments were performed in a murine system to elucidate species-dependent differences. An analysis of cytokine production was performed to determine whether heparin facilitates noncanonical IL-12 signaling. Finally, data gathered were used to propose a working model for heparin-induced stabilization of IL-12/IL-12R, which was visualized with molecular graphics software.

## Results

### Heparin modulates hIL-12 bioactivity in a dose-dependent manner

The effect of heparin concentration on hIL-12 activity was quantified via interferon- $\gamma$  (IFN- $\gamma$ ) production by NK-92MI cells, activated human T cells, or activation of signaling in HEK-Blue<sup>TM</sup> IL-12 cells. There were significant increases in hIL-12-induced activities in the presence of heparin for all cell types tested. In detail, IFN- $\gamma$  production by NK-92MI cells in response to 200 pg/ml hIL-12 more than doubled from  $4.438 \pm 0.479$  to  $7.876 \pm 0.395$  ng/ml as exogenous heparin concentration increased from 0 to 25  $\mu$ g/ml (Fig. 1A). Additional heparin, beyond 25  $\mu$ g/ml, produced no further increase in hIL-12 activity, indicating a potential plateau. HEK-Blue<sup>TM</sup> IL-12 cells and T cells responded similarly with increasing levels of heparin inducing enhanced hIL-12 bioactivity (Fig. 1, B and C). At very high heparin concentrations (100 and 500  $\mu$ g/ml), there was a

decrease in hIL-12 bioactivity in the HEK-Blue<sup>TM</sup> IL-12 cells indicating a possible inhibitory effect.

Unlike in the human system, heparin did not enhance the activity of mIL-12 on either murine 2D6 cells (Fig. 1D) or splenocytes isolated from C57BL/6J mice (Fig. 1E). Interestingly, heparin significantly enhanced the activity of mIL-12 on human NK cells (Fig. 1F). Heparin facilitated a 1.55-fold increase in mIL-12 function on human NK cells which was greater than the heparin-induced 1.18-fold increase in hIL-12 function on human NK cells (Fig. 1F). Conversely, hIL-12 was not active in the murine 2D6 cell line with or without heparin (Fig. 1E).

### Heparin does not facilitate noncanonical hIL-12 signaling

IFN- $\gamma$  expression is a key indicator of hIL-12 bioactivity. However, it is possible that heparin facilitated expression of other T helper cytokines via noncanonical signaling. Thus, we investigated the production of prototype Th1, Th2, and Th17 cytokines by NK-92MI cells and activated T cells exposed to hIL-12 with and without exogenous heparin. As expected, in response to hIL-12 alone, NK-92MI cells secreted high levels of IFN- $\gamma$  ( $663.5 \pm 4.9$  pg/ml), whereas heparin alone had no effect (Fig. 2A). Treatment with hIL-12 alone also increased the production of IL-10 and IL-6 by NK-92MI cells, which was similarly reported by another group (23). Upon addition of heparin, NK-92MI significantly increased production of IFN- $\gamma$ , IL-10, and IL-6 by 1.26-, 1.47-, and 1.92-fold (Fig. 2A), respectively. It should be noted that IL-2 was detected in all treatment groups because the NK92-MI cell line is stably transfected with the IL-2 gene to maintain consistent cell proliferation (24). The amount of IL-2 did not change significantly with the addition of heparin. NK-92MI did not produce significant amounts of TNF $\alpha$ , IL-4, or IL-17A regardless of hIL-12 or heparin treatment (Fig. S3, A and C). Activated T cells produced  $626.8 \pm 2.4$  pg/ml of IFN- $\gamma$  in response to hIL-12. This was increased to  $1031.9 \pm 27.9$  pg/ml when heparin was included (Fig. 2B). No other cytokine was secreted by activated T cells in response to heparin, hIL-12, or their combination (Fig. S3, B and D).

To document possible changes in the frequencies of IFN- $\gamma$ -producing cells, we investigated the intracellular expression of IFN- $\gamma$  by CD4<sup>+</sup> T cells, CD8<sup>+</sup> T cells, and CD56<sup>+</sup> cells in PBMCs and NK92-MI cells in response to hIL-12 alone and hIL-12 plus heparin. The results showed that the combination of hIL-12 and heparin increased the percentages of cells producing IFN- $\gamma$  over hIL-12 alone (CD4<sup>+</sup> T cells: from  $2.633 \pm 0.291$  to  $4.207 \pm 0.522\%$ ; CD8<sup>+</sup> T cells: from  $1.757 \pm 0.378$  to  $3.597 \pm 0.616\%$ ; CD56<sup>+</sup> NK cells: from  $2.293 \pm 0.040$  to  $3.103 \pm 0.496\%$ ; and NK-92MI cells: from  $1.473 \pm 0.163$  to  $9.810 \pm 0.132\%$ ) (Fig. 2, C–E).

### EC<sub>50</sub> of IL-12 is reduced by heparin

The ability of heparin to reduce the half-maximal effective concentration (EC<sub>50</sub>) of IL-12 was quantified in NK-92MI cells, human T cells, and PBMCs. Supernatants from cells treated with increasing concentrations of hIL-12, with or without heparin, showed a typical sigmoidal dose-response relationship (Fig. 3). The EC<sub>50</sub> values, calculated by Graphpad Prism 7, for IL-12 alone and IL-12 with heparin were 27.67 and 2.34 pg/ml,

<sup>5</sup> K. G. Nguyen, F. B. Gillam, J. J. Hopkins, S. Jayanthi, R. K. Gundampati, G. Su, J. Bear, G. R. Pilkington, R. Jalal, B. K. Felber, J. Liu, S. K. Thallapuram, and D. A. Zaharoff, unpublished data.

## Mechanisms of heparin-induced IL-12 modulation

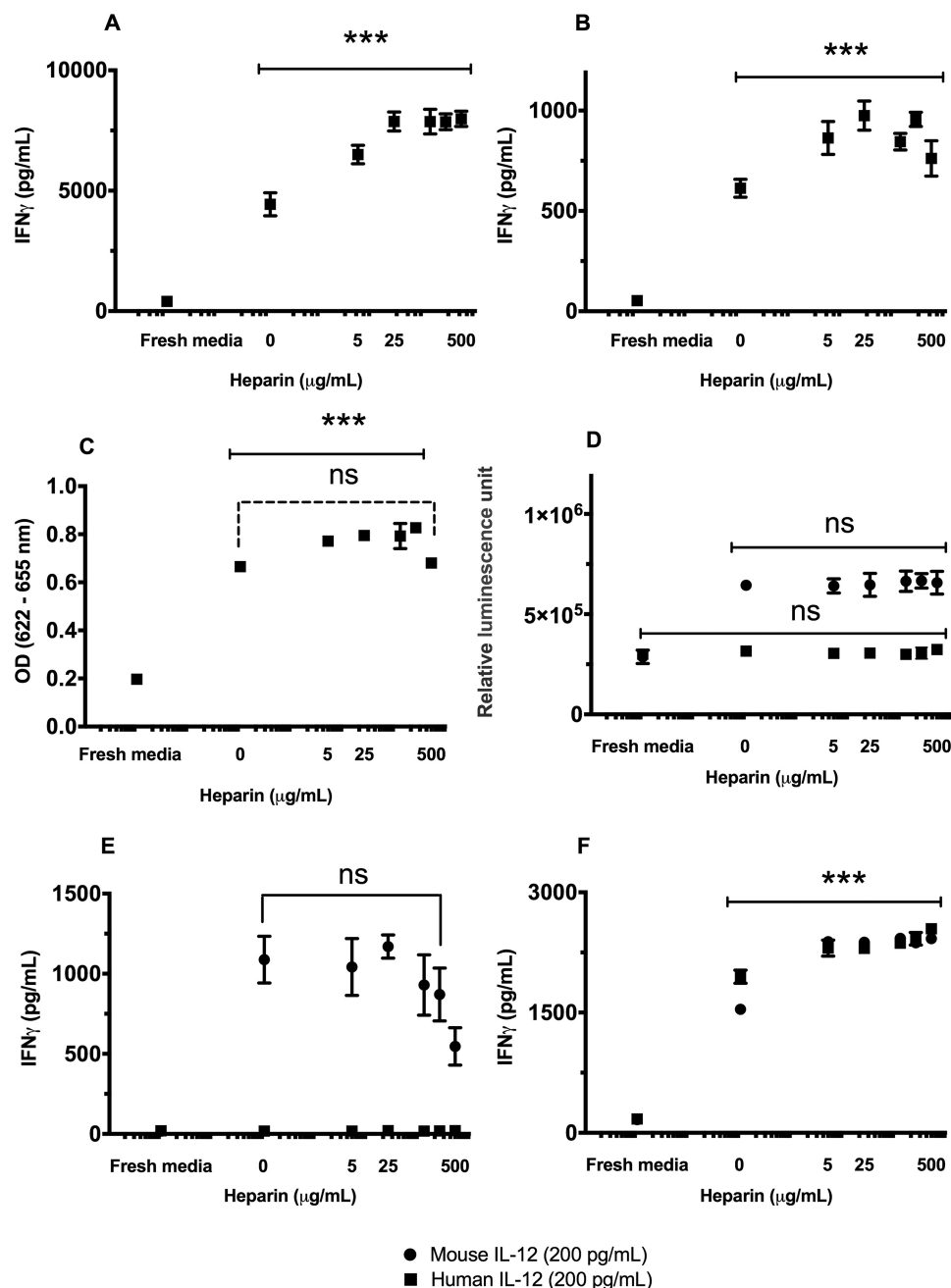


**Figure 1. IL-12 bioactivity is modulated by heparin in a dose-dependent manner.** The production of IFN- $\gamma$  by NK-92MI cells (A) or human T cells (B) or alkaline phosphatase by HEK-Blue™ IL-12 cells (C) was measured after exposure to a fixed concentration of hIL-12, 200 pg/ml for A and B, or 1 ng/ml for C, and increasing concentrations of heparin. D, proliferation of mIL-12 sensitive 2D6 cells in response to mIL-12 and hIL-12 with increasing heparin concentrations was indirectly assessed via CellTiter-Glo® 3D Cell Viability Assay. IFN- $\gamma$  production by murine splenocytes isolated from C57BL/6J mouse (E) and NK-92MI cells in response to mIL-12 and hIL-12 with increasing heparin concentrations (F) was measured via ELISA. Asterisks indicate a significant difference between the treatments of IL-12 alone and IL-12 plus increasing heparin concentrations (\*\*,  $p < 0.01$ , and \*\*\*,  $p < 0.001$ , via one-way ANOVA; solid lines); ns, not significant. The comparison of IL-12 bioactivity in response to hIL-12 alone and different heparin concentrations plus hIL-12 (200 pg/ml) was evaluated by Tukey's post-test (dashed lines). Data points represent mean  $\pm$  S.D. of triplicate measurements. Experiments were performed in triplicate and repeated three times with similar results.

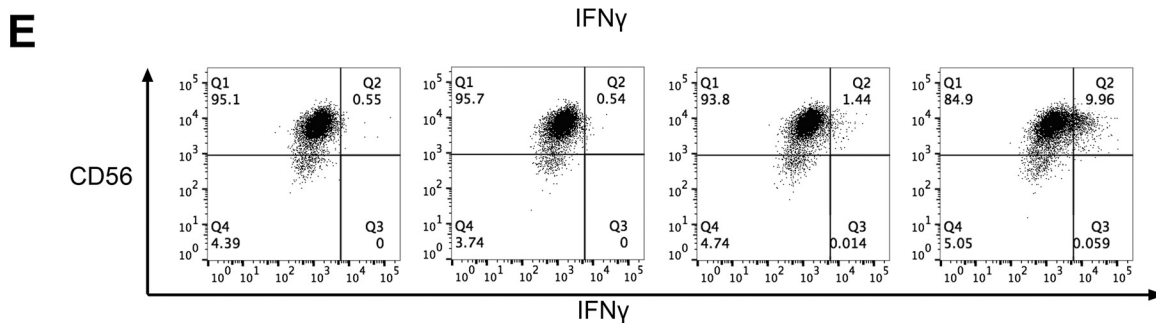
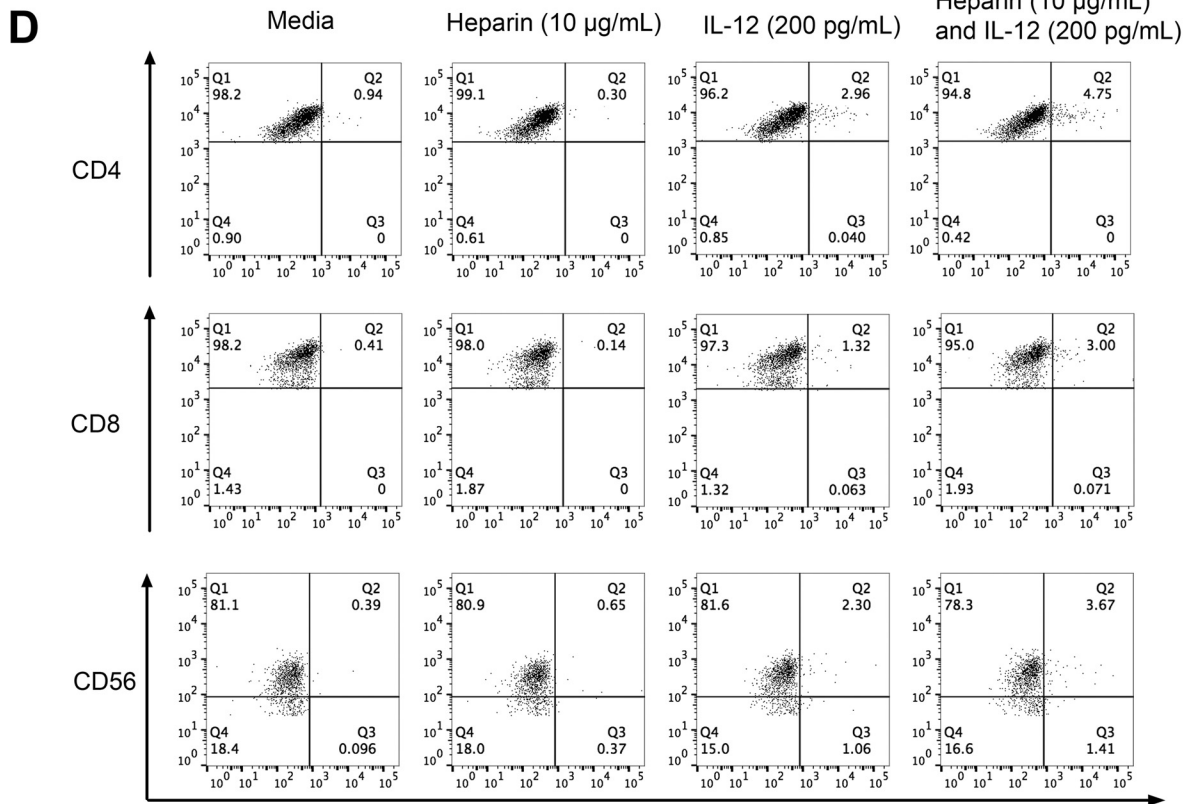
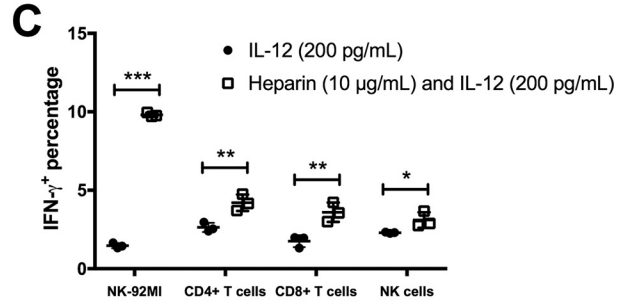
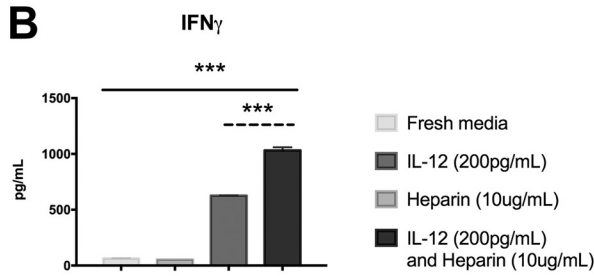
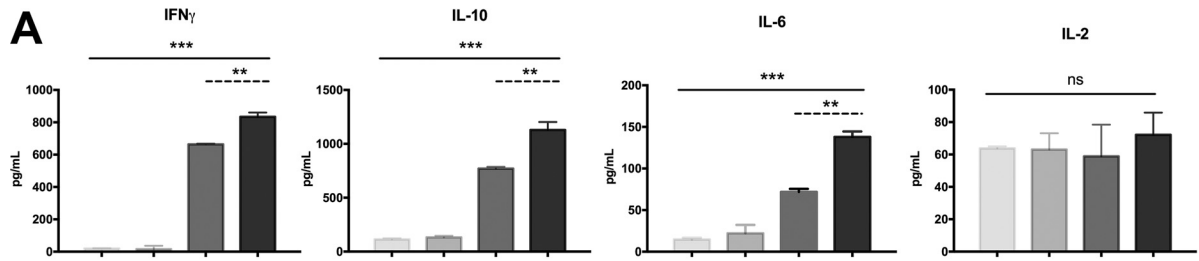
respectively. Based on this result, heparin decreased the  $EC_{50}$  of IL-12 by 11.8-fold. Similar results were observed on human T cells and PBMCs that showed a reduction in  $EC_{50}$  value of hIL-12 from 324.5 to 220.2 pg/ml, or 1.5-fold, and from 121.9 to 13.76 pg/ml, or 8.9-fold, respectively.

### Effect of heparin chain length on IL-12 binding

ITC measures thermodynamic changes associated with the interactions between molecules in solution. These measure-

ments can be used to determine thermodynamic parameters such as binding affinity, change in enthalpy, and stoichiometry between interacting molecules. The interaction of heparin with mIL-12 or hIL-12 is exothermic. Under the experimental conditions used, the binding isotherms are observed to be hyperbolic, and heparin binds to both hIL-12 and mIL-12 nearly in a 1:1 stoichiometry. Analysis of ITC data indicate that the binding affinity ( $K_d$ (apparent)) of heparin-IL-12 interaction is strongly influenced by the chain length of heparin (Fig. 4). Spe-

# Mechanisms of heparin-induced IL-12 modulation





## Mechanisms of heparin-induced IL-12 modulation

cifically, heparin oligosaccharides with fewer than six saccharide units, like heparin di-, tetra-, and hexasaccharide, do not exhibit significantly binding to either hIL-12 or mL-12 (Table 1). Heparin octasaccharide shows reasonably strong binding ( $K_d(\text{apparent}) = 39.7 \pm 3.2 \mu\text{M}$ ) to hIL-12 but not to mL-12 (Table 1 and Fig. 4). The binding affinities of longer chain length heparin oligosaccharides, heparin decasaccharide and heparin dodecasaccharide, to IL-12 are the strongest and range from  $5.2 \pm 0.1$  to  $9.0 \pm 0.4 \mu\text{M}$  (Table 1). The binding affinity of hIL-12 and mL-12 to LMWH, which is a polydisperse mixture of heparin with varying lengths of saccharide units, is  $9.8 \pm 0.2$  and  $45.2 \pm 1.1 \mu\text{M}$ , respectively.

In summary, ITC data demonstrate that hIL-12, in general, exhibits lower  $K_d$  values and thus higher binding affinities to heparin molecules than mL-12. In addition, the binding affinity between hIL-12 and heparin increases with heparin chain length and reached a maximum with heparin dodecasaccharide. The binding affinity between hIL-12 and LMWH was lower than heparin dodecasaccharide as LMWH also contains a number of shorter heparin fragments, which likely compete with longer heparin chains.

### Heparin-induced modulation of hIL-12 bioactivity depends on heparin's chain length

The effect of heparin's chain length on hIL-12 bioactivity was investigated in NK-92MI cells and HEK-Blue<sup>TM</sup> IL-12 cells. IFN- $\gamma$  production data from NK-92MI cells showed that tetrasaccharides did not enhance hIL-12 bioactivity, whereas hexasaccharides generated a modest enhancing effect (Fig. 4A). hIL-12 activity was further increased in the presence of heparin octasaccharides and reached a plateau with decasaccharides and dodecasaccharides. LMWH, which is typically 15–25 saccharide units, produced similar enhancements in hIL-12 bioactivity (Fig. 4A). A comparable plateau phenomenon with heparin decasaccharides and dodecasaccharides was observed with HEK-Blue<sup>TM</sup> IL-12 cells (Fig. 4B).

### Effect of sulfation on IL-12-HS binding

To determine how sulfation level affects heparin binding to IL-12, a novel microarray approach was used. Fifty two heparan sulfate (HS)-derived compounds were synthesized with 1, 2, or 3 sulfate groups per disaccharide unit ranging in size from 5 to 18 saccharides (Fig. S4). The compounds were arrayed on a slide and treated with fluorescence-labeled IL-12. After rinsing, a fluorescence analysis was performed to quantify levels of IL-12 binding to each of the HS-derived compounds. Our analysis revealed that the highest amounts of hIL-12 were bound to

HS-derived compounds 18 and 19, which contain the maximum of three sulfate groups per disaccharide unit (Fig. 5A). Similar results were found when mL-12 was tested (Fig. 5B). Once again, mL-12 was found to bind strongest to compounds 18 and 19 and to a lesser degree to compounds 20 and 22, which contained two sulfates per disaccharide. It should be noted that the large *bright-green circles* shown on the microarray were artifacts and were not included in our analysis (Fig. 5B). Other sulfated heparin-derived compounds also bound and retained IL-12, however, at significantly lower levels. Taken together, these data indicate that sulfation level is a key factor in the binding of sulfated GAGs to IL-12.

### Sulfation is essential for HS-induced modulation of hIL-12 bioactivity

To determine the effect of sulfation level on the modulation of hIL-12 bioactivity by heparin, selected HS dodecasaccharides containing 1, 2, or 3 sulfate groups per disaccharide unit were selected (Fig. S4) and formulated with hIL-12 for treatment on NK-92MI cells and HEK-Blue<sup>TM</sup> IL-12 cells. Data from NK-92MI cells showed that compounds 21–25, which contained less than three sulfate groups per disaccharide and did not substantially bind hIL-12, also did not enhance hIL-12 bioactivity (Fig. 5, B and C). In contrast, compounds 18 and 19, which consisted of three sulfate groups per disaccharide unit, significantly enhanced hIL-12 bioactivity to levels similar to LMWH. Data from HEK-Blue<sup>TM</sup> IL-12 cells exhibited similar phenomena in that hIL-12 activity was only enhanced with compounds 18 and 19. It should be noted that compound 23 produced different effects on IL-12 bioactivity in NK-92MI cells and HEK-Blue<sup>TM</sup> IL-12 cells indicating that certain HS enhancement phenomena may be cell-dependent.

### Proposed model of heparin-stabilized hIL-12/hIL-12R complex

The structure of hIL-12 was imported from the PDB archive (1F45) (Fig. 6A). The heparin docking function in ClusPro was used to identify two high-scoring heparin-binding motifs on the p40 subunit of hIL-12 (<sup>117</sup>LKDQKEPKNK<sup>126</sup> and <sup>276</sup>QVQGKSKREKK<sup>286</sup>) (Fig. 6A). These correlate with our previous *in silico* analysis (15).

Models of each receptor subunit were based on the solved structure of interleukin-6 receptor subunit  $\beta$  with differences. hIL-12R $\beta$ 1 was also based on the structures of anosmin-1, leukemia inhibitory factor receptor, and insulin receptor. The structure of hIL-12R $\beta$ 2 was further detailed using homology to human receptor 2 protein-tyrosine phosphatase  $\sigma$ , chicken mdga1, and the ectodomain of the re-

**Figure 2. Heparin amplifies hIL-12-induced cytokine profiles.** The production of prototypical Th1, Th2, and Th17 cytokines by NK-92MI cells (A) and T cells (B) in response to hIL-12 (200 pg/ml) in the presence and absence of heparin (10  $\mu\text{g}/\text{ml}$ ) were analyzed via a cytometric bead array kit (BD Biosciences). Heparin alone does not alter baseline cytokine production, whereas the addition of heparin to hIL-12 increases the amount but does not alter the type of cytokine expressed by NK or T cells. Columns represent mean  $\pm$  S.D. of triplicate measurements. C, dot plots show representative expression of IFN- $\gamma$  by gated CD3<sup>+</sup> CD4<sup>+</sup> T cells, CD3<sup>+</sup> CD8<sup>+</sup> T cells, and CD3<sup>-</sup> CD56<sup>+</sup> NK cells from PBMCs in four experimental groups (fresh media, heparin, hIL-12, and hIL-12 plus heparin). D, dot plots show representative expression of IFN- $\gamma$  by gated CD56<sup>+</sup> NK92-MI cells in four experimental groups (fresh media, heparin, hIL-12, and hIL-12 plus heparin). E, dot plots describe positive percentages of intracellular IFN- $\gamma$  in NK-92MI cells, CD4<sup>+</sup> T cells, CD8<sup>+</sup> T cells, and NK cells for comparison of hIL-12 alone and hIL-12 plus heparin (\*,  $p < 0.05$ ; \*\*,  $p < 0.01$ ; and \*\*\*,  $p < 0.0001$  via two-tailed *t* test). A and B, asterisks (\*\*,  $p < 0.01$ , and \*\*\*,  $p < 0.001$ ) indicate a significant difference between the treatments of fresh media, heparin alone, IL-12 alone, and IL-12 plus heparin via one-way ANOVA (solid lines); ns, not significant. The comparison of IL-12 bioactivity in response to hIL-12 alone and different heparin concentrations plus hIL-12 (200 pg/ml) was evaluated by Tukey's post-test (dashed lines). Data points represent mean  $\pm$  S.D. of triplicate measurements. Experiments were performed in triplicate and repeated three times with similar results.

## Mechanisms of heparin-induced IL-12 modulation

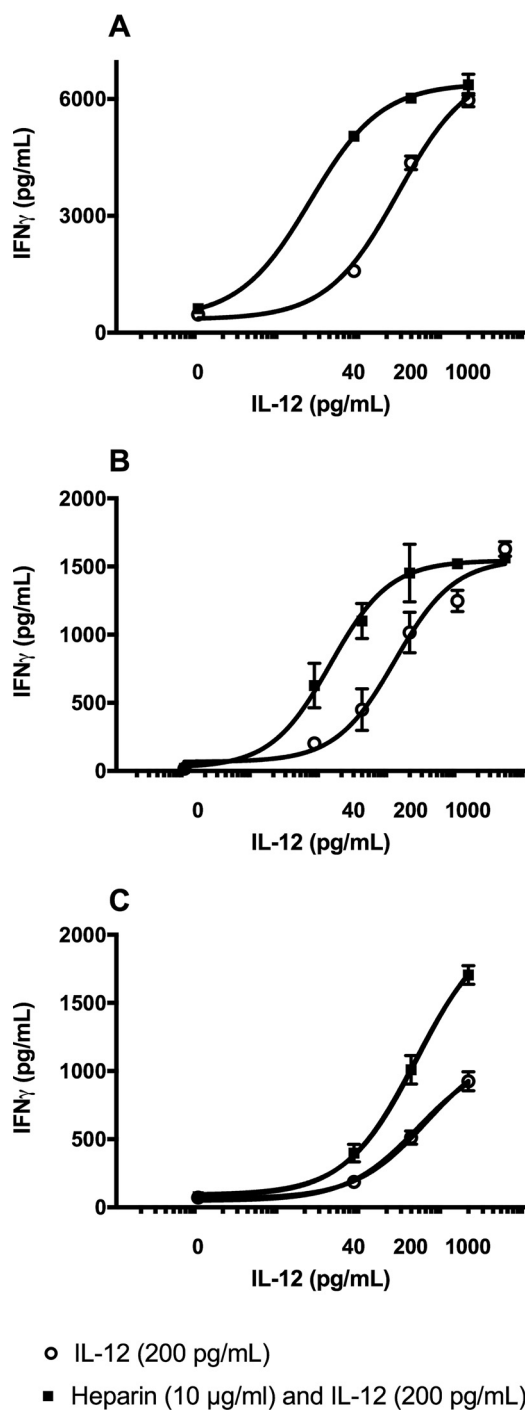


**Figure 3. Heparin decreases the  $EC_{50}$  value of hIL-12.** hIL-12 bioactivity curves showing the IFN- $\gamma$  production by NK-92MI cells (A), human PBMCs (B), and human T cells (C) exposed to increasing hIL-12 in the presence and absence of heparin (10  $\mu$ g/ml). The  $EC_{50}$  values of hIL-12 for NK-92MI cells and human PBMCs were significantly decreased by heparin ( $p < 0.0001$  versus hIL-12 alone via extra sum-of-squares  $F$  test). All data points represent mean  $\pm$  S.D. of triplicate measurements. Experiments were performed in triplicate and repeated three times with similar results.

ceptor protein-tyrosine 2 phosphatase  $\mu$ . Each prediction showed high (>90%) confidence in the model. Heparin-binding segments on receptor subunit ECDs were predicted using ClusPro. The top-scoring segment for each receptor subunit was identified and highlighted in the protein models (Fig. 6, B and C).

To determine the spatial relationship of the heparin-binding segments and the potential role of heparin in stabilizing ligand-receptor interactions, we constructed a model of the hIL-12/hIL-12R complex using the available crystal structure of hIL-12 and its predicted binding to the ECDs (Fig. 6, D and E). The predicted hIL-12/hIL-12R complex shows the heparin-binding motifs located on hIL-12 to be in close proximity to hIL-12R $\beta$ 1. Estimated distances from the heparin-binding sites on hIL-12 to the putative heparin-binding site on hIL-12R $\beta$ 1 were 14 and 18 Å (Fig. 6F). For the hIL-12R $\beta$ 2 ECD, the heparin-binding site is facing away from the p35 subunit of hIL-12. Consequently, the distances from the heparin-binding sites on hIL-12 to the top-scoring heparin-binding site on hIL-12R $\beta$ 2 were longer at 43 and 75 Å. Based on the putative heparin-binding sites, this model predicts that only heparin molecules of a certain size could simultaneously bind to both the IL-12 ligand and receptor. Using an average length of 4 Å per disaccharide, it becomes clear that only heparin molecules with chain lengths of 4, 5, or 6 disaccharide units, *i.e.* 8, 10, or 12 saccharides, are able to consistently bridge the heparin-binding domains. In addition, the increased binding and activities observed with higher sulfation levels indicate that the stabilization interaction is likely mediated by nonspecific electrostatic interactions and not particular sulfation patterns.

## Discussion

Our previous study was the first to demonstrate that sulfated GAGs, such as heparin and heparan sulfate, could enhance the bioactivity of hIL-12 (17). In this follow-up study, we extended this research to identify the characteristics of heparin that were required to modulate hIL-12 bioactivity. In doing so, we aimed to develop a working model capable of explaining the mechanism(s) of heparin-induced hIL-12-enhanced function.

Initial studies to determine the optimal concentration of heparin found that, for most cell types, a maximal or plateau effect was achieved between 10 and 25  $\mu$ g/ml heparin (Fig. 1). These concentrations are considered physiologically relevant as circulating levels of heparin in humans are 1–5  $\mu$ g/ml (25). During inflammation, systemic concentrations of heparin and heparan sulfate are significantly increased (26, 27). Although not explored, we hypothesize that local sites of inflammation have similar increases in heparin and heparan sulfate.

Because our previous study demonstrated that heparin can recover IL-12 signaling in cells lacking functional IL-12 receptors (17), we hypothesized that IL-12 could be signaling through noncanonical pathways, perhaps via receptors associated with other IL-12 family members. However, our cytokine-profiling analyses and intracellular cytokine staining showed that no other Th1, Th2, or Th17 cytokines were induced in the presence of heparin (Fig. 2). Heparin simply appears to make hIL-12 signaling more efficient. In particular, a greater percentage of lymphocytes respond to hIL-12 in the presence of heparin (Fig. 2, C and D). Also, the  $EC_{50}$  data demonstrated that heparin can reduce the effective concentration of hIL-12 by 1.5- to 11.8-fold (Fig. 3).

In terms of heparin characteristics, both chain length and sulfation level exhibited a threshold-type effect on hIL-12. Specifically, heparin molecules less than a threshold of six saccha-

## Mechanisms of heparin-induced IL-12 modulation

ride units did not affect hIL-12 activity, whereas those above eight saccharide units induced a bioactivity plateau that was similar to LMWH (Fig. 4). It should be noted that heparin hexasac-

charides, which only modestly enhanced hIL-12 activity, were not found to bind strongly to hIL-12 in ITC studies. This apparent discrepancy may be due to differences in sensitivity between

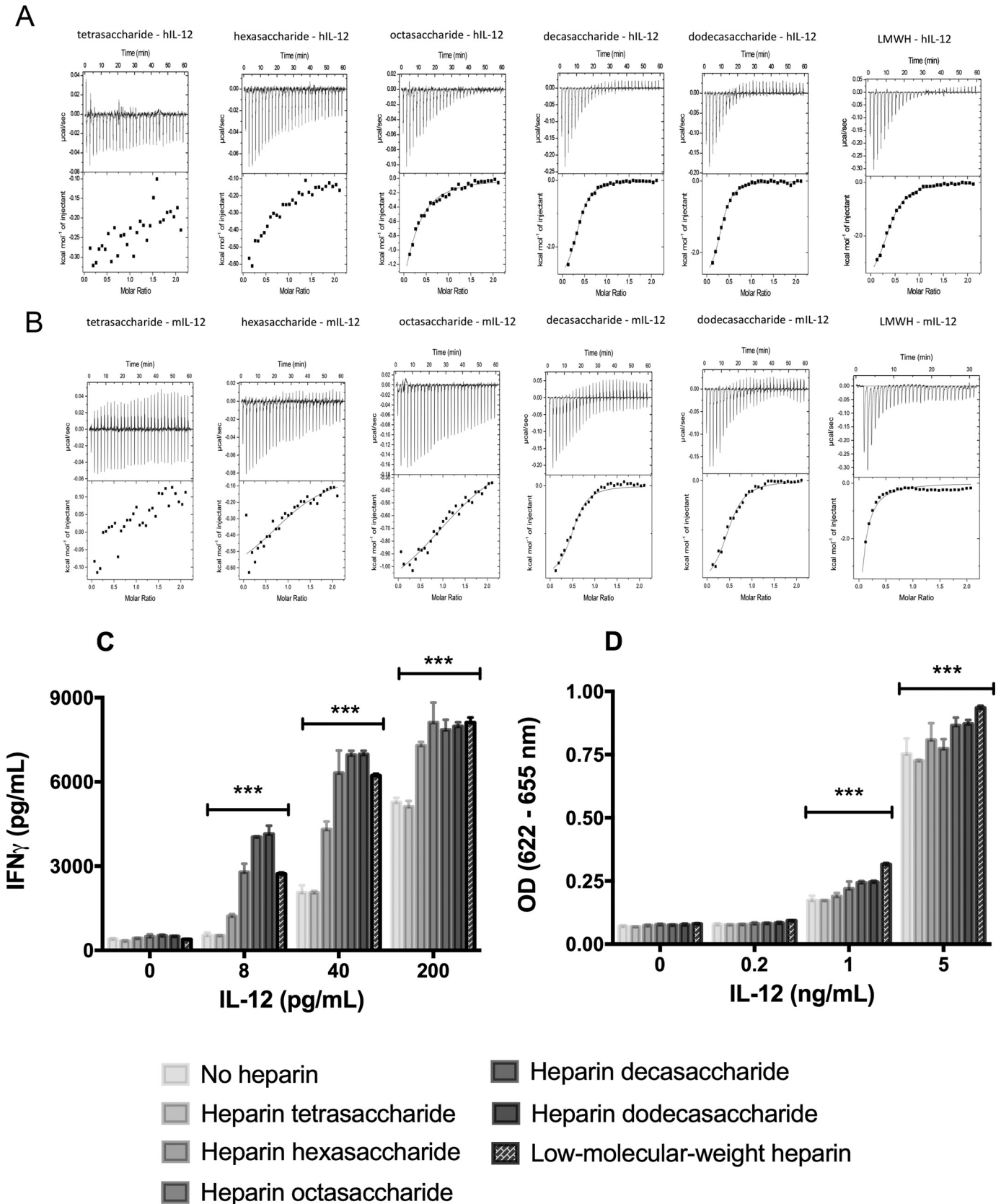




**Table 1****Binding affinities (mean  $\pm$  S.D.) between hIL-12 or mL-12 and heparin oligosaccharides or LMWH**

NB means no binding was observed.

	Tetra-saccharide	Hexa-saccharide	Octa-saccharide	Deca-saccharide	Dodeca-saccharide	LMWH
hIL-12	NB	NB	39.7 $\pm$ 3.2 <sup><math>\mu</math>M</sup>	6.5 $\pm$ 0.2 <sup><math>\mu</math>M</sup>	5.2 $\pm$ 0.1 <sup><math>\mu</math>M</sup>	9.8 $\pm$ 0.2 <sup><math>\mu</math>M</sup>
mIL-12	NB	NB	NB	6.1 $\pm$ 0.4	9.0 $\pm$ 0.4 <sup>a</sup>	45.2 $\pm$ 1.1 <sup>a</sup>

<sup>a</sup>  $p < 0.0001$  compared with hIL-12 and mL-12 via two-tailed  $t$ -test.

the two approaches. ITC requires higher concentrations of heparin and hIL-12, whereas the limit of reliable detection of binding is on the order of a couple hundred micromolars. Thus, heparin hexasaccharide binding to hIL-12 may be too weak to be detected but still strong enough to provide partial enhancement of hIL-12 activity.

Regarding the effects of sulfation, HS-derived compounds with less than three sulfate groups per disaccharide did not significantly improve hIL-12 bioactivity. In contrast, both HS molecules containing three sulfate groups showed improved hIL-12 binding and bioactivity (Fig. 5). In the murine system, a similar influence of sulfation was found in binding studies (Fig. 5); however, sulfated GAGs do not appear to enhance the activity of mL-12 in mouse lymphocytes (Fig. 1E). Mechanistically, HS-derived molecules with less than three sulfate groups per disaccharide have lower negative charge densities which likely results in weaker interactions with both hIL-12 and hIL-12R. These data imply that the heparin–IL-12 interaction is a non-specific electrostatic interaction as opposed to an interaction that depends on a particular sulfation pattern. The inability of poorly sulfated HS to enhance hIL-12 bioactivity agreed with our previous data demonstrating that poorly or nonsulfated GAGs, e.g. chondroitin sulfate and hyaluronic acid, had no effect on hIL-12 bioactivity (17).

Using the chain length data in particular, we hypothesized that heparin could be stabilizing the hIL-12/hIL-12R complex by binding to heparin-binding domains on both ligand and receptor. We reasoned that only heparin molecules of a sufficient size would be able to bind simultaneously to heparin-binding sites on different subunits of the complex. Our *in silico* analysis identified two major heparin-binding domains on hIL-12 as well as the top-scoring heparin-binding segments on each hIL-12R subunit (Fig. 6). When hIL-12 is bound to IL-12R, the distances between heparin-binding domains located on different proteins, *i.e.* IL-12, IL-12R $\beta$ 1 and IL-12R $\beta$ 2, range from 14 to 75 Å. A tetrasaccharide, with a maximum distance of  $\sim$ 16–17 Å between sulfate groups, would therefore have a lower probability of binding to and stabilizing the hIL-12–hIL-12R interactions than an octasaccharide or LMWH.

It should be noted that the tertiary complex and the identified heparin-binding domains on hIL-12, IL-12R $\beta$ 1, and

IL-12R $\beta$ 2 are merely predictions at this point. However, Garnier *et al.* (16) demonstrated that truncation of the carboxyl-terminal domain on the p40 subunit to exclude the putative heparin-binding segment located within amino acids 279–287 significantly reduced the heparin-binding ability of hIL-12. Where exactly heparin binds to IL-12, both human and mouse, as well as each IL-12R subunit is the subject of ongoing crystallography work. Once completed, we will have a definitive picture of the heparin/IL-12/IL-12R quaternary complex.

An observation that appears to agree with our stabilization hypothesis was that heparin did not improve mL-12 bioactivity on mouse 2D6 cells, but significantly improved mL-12 bioactivity on human NK-92MI cells (Fig. 1). It is possible that the binding of mL-12 to mL-12R is of sufficient affinity such that heparin is not needed to enhance binding and signaling. In contrast, the affinity of mL-12 for hIL-12R is expected to be much lower than the affinity of mL-12 for mL-12R or hIL-12 for hIL-12R. Therefore, the benefit of adding heparin to stabilize the potentially “loose” mL-12/hIL-12R complex results in a robust enhancement of mL-12 activity. In fact, the activity of mL-12 was increased 1.55-fold, which was greater than heparin-induced enhancements for hIL-12 (1.18-fold) (Fig. 1D).

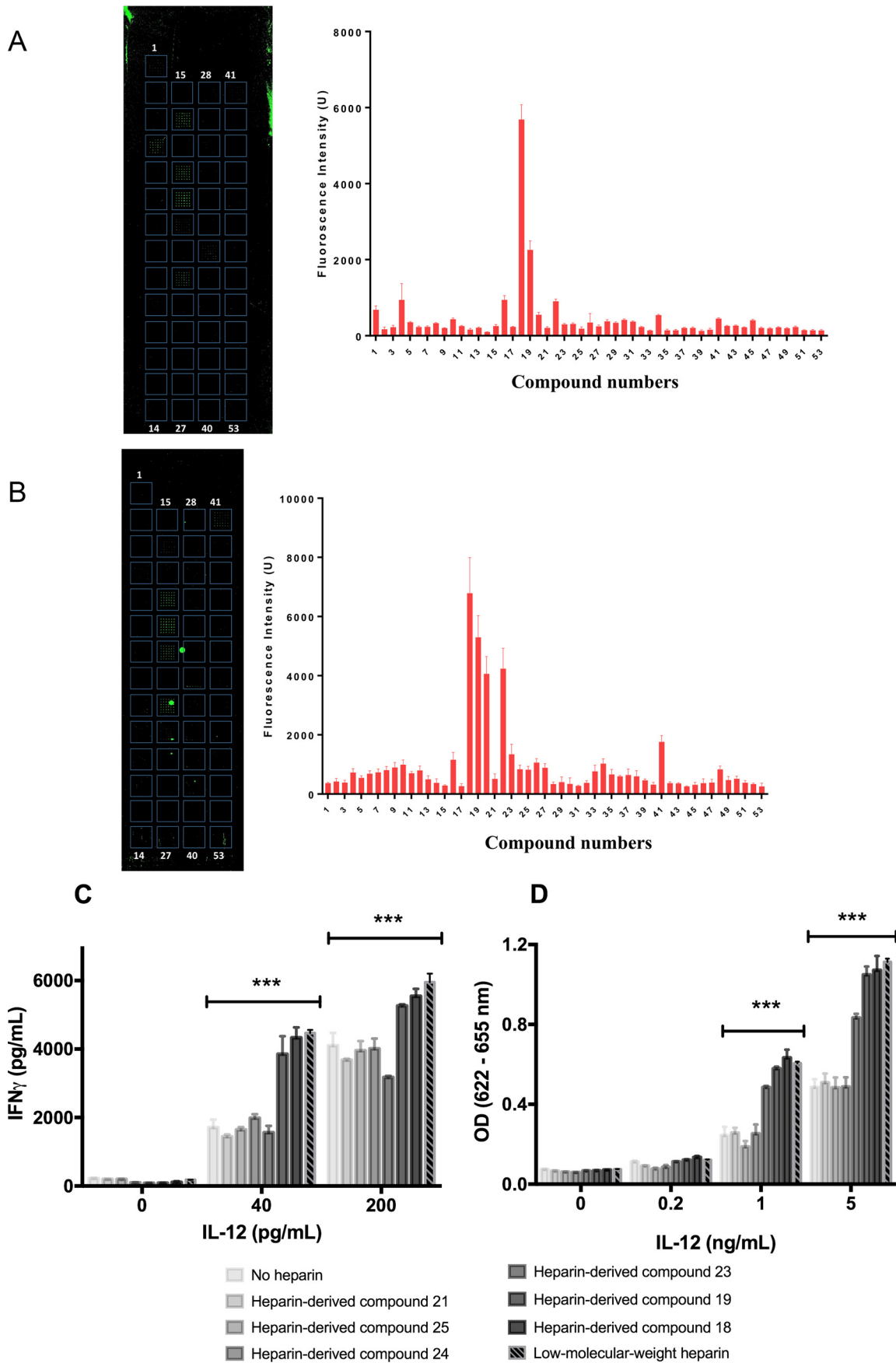
Drawing from our previous work, heparin’s ability to stabilize weak IL-12–IL-12R interactions may be a key mechanism by which hIL-12 signaling was recovered in cells lacking functional hIL-12R (17). In these previous studies, hIL-12R $\beta$ 1 and hIL-12R $\beta$ 2 were functionally deleted via CRISPR/Cas9 genome editing. However, the Cas9-induced cleavage of the IL-12R $\beta$ 1 and IL-12R $\beta$ 2 genes likely induced random mutations in the receptor subunits instead of a complete knockout. The mutated hIL-12R did not bind hIL-12 sufficiently to allow signaling; however, the addition of heparin may have stabilized this loose complex enough to recover hIL-12 bioactivity. Ongoing studies are aimed at understanding which portions of the IL-12R subunits are critical for signaling in the presence and absence of heparin. We postulate that this research will lead to a new therapeutic option for patients with mutations in IL-12R $\beta$ 1 that lead to Mendelian susceptibility to mycobacterial diseases (28, 29).

Finally, other heterodimeric cytokines of the IL-12 family have overlapping structural features (30) and therefore could be

**Figure 4. Modulatory activity depends on heparin chain length.** Isothermograms describe binding interactions between heparin and hIL-12 (A) or mL-12 (B). The upper panel of each isothermogram shows the raw data obtained for each of the 30 injections. The lower panels display the best fit data to one-set of sites binding model using Origin™ version 7.0 software. hIL-12 activity as measured by IFN- $\gamma$  production by NK-92MI cells (C) or secreted alkaline phosphatase by HEK-Blue™ IL-12 cells (D) was measured after co-culture with heparin oligosaccharides or LMWH (10  $\mu$ g/ml). Heparin octasaccharide, decasaccharide, dodecasaccharide, and LMWH significantly increased the bioactivity of IL-12 in NK-92MI cells and HEK-Blue™ IL-12 cells (\*\*\*,  $p < 0.0001$  versus hIL-12 alone via two-way ANOVA). Heparin tetrasaccharide did not increase the bioactivity of hIL-12 in NK-92MI cells ( $p > 0.05$  versus hIL-12 alone via Tukey’s post-test) and HEK-Blue™ IL-12 cells ( $p < 0.0001$  versus hIL-12 alone via Tukey’s post-test). Heparin hexasaccharide increased the bioactivity of hIL-12 in NK-92MI cells ( $p < 0.0001$  versus hIL-12 alone,  $p < 0.01$  versus hIL-12 plus LMWH via Tukey’s post-test) and showed no effect on hIL-12 bioactivity in HEK-Blue™ IL-12 cells ( $p > 0.05$  versus hIL-12 alone via Tukey’s post-test). Columns represent mean  $\pm$  S.D. of triplicate measurements. Experiments were performed in triplicate and repeated three times with similar results.



# Mechanisms of heparin-induced IL-12 modulation



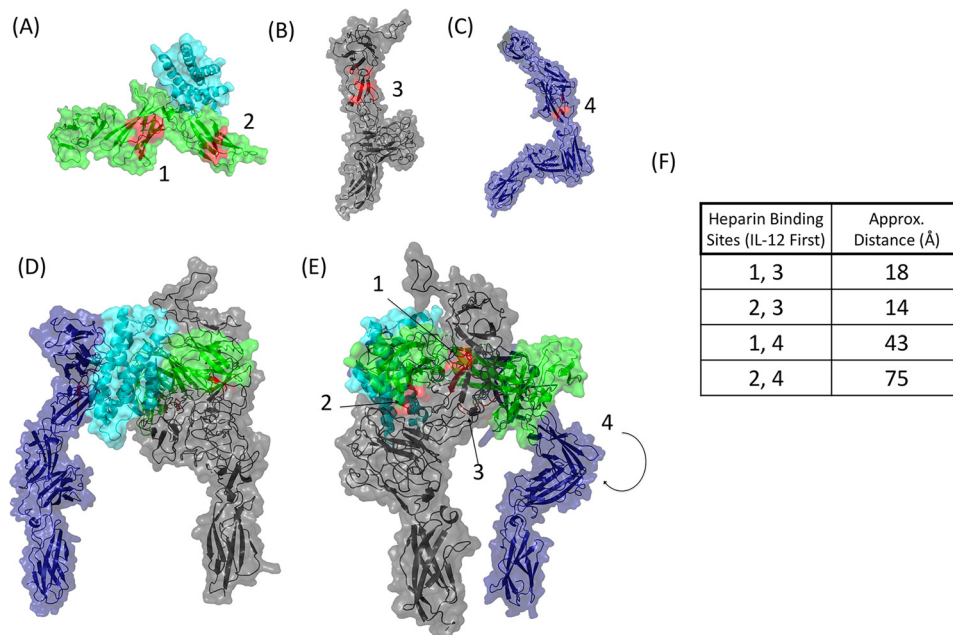


**Figure 6. Heparin may stabilize the interactions of hIL-12 with hIL-12R $\beta$ 1 and hIL-12R $\beta$ 2.** A, heparin-binding motifs (red) on hIL-12 (PDB code 1F45) were identified in ClusPro as <sup>117</sup>LKDQKEPKNK<sup>126</sup> and <sup>276</sup>QVQGKSKREKK<sup>286</sup>. The ECD structures of hIL-12R $\beta$ 1 (B) and hIL-12R $\beta$ 2 (C) were modeled in PyMOL. As with hIL-12, heparin-binding segments for each receptor subunit were identified in ClusPro. The top-scoring segment for each subunit is highlighted (red). D, model of the hIL-12/hIL-12R complex was predicted using PyMOL and ClusPro. Two views of the model, rotated nearly 180° around the vertical axis, relate the locations of the heparin binding segments (red). E, estimated distances from each of the heparin-binding sites on hIL-12 to the putative heparin-binding sites on the receptor subunits were calculated using PyMOL's measurement tool.

modulated by heparin. In particular, IL-23 shares the p40 subunit along with its cognate receptor IL-12R $\beta$ 1 with IL-12. IL-35 shares p35 and IL-12R $\beta$ 2 with IL-12. Our preliminary data indicate that heparin's enhancement of hIL-23 bioactivity is even more robust than its effects on hIL-12 (data not shown). Given the diverse immunological functions of the IL-12 family, the impact of heparin as a regulator of immunity is of great interest.

## Experimental procedures

### Mice

Eight- to ten-week-old female C57BL/6J mice were purchased from The Jackson Laboratory (Bar Harbor, ME). Animal use was in compliance with the Public Health Service Policy on Humane Care and Use of Laboratory Animals. All experiments involving laboratory animals were approved by the Institutional Animal Care and Use Committee at North Carolina State University.

### Recombinant proteins and heparin compounds

Recombinant hIL-12 was purified from hIL-12-expressing HEK293 cells as described previously (15). Recombinant mIL-12 was overexpressed by HEK293 cells stably transfected with optimized mIL-12p70 plasmid (AG250) (13). IL-12-producing

HEK293 cells were grown in serum-free media in a Hollow Fiber bioreactor that allows high-density growth without any animal components. mIL-12 was purified via heparin-Sepharose chromatography as described previously (15). mIL-12 cytokine production was quantified via ELISA (ThermoFisher Scientific mouse IL-12p70 ELISA; catalogue no. BMS6004). Recombinant hIL-12 was purchased from PeproTech (Rocky Hill, NJ). LMWH and heparin oligosaccharides were purchased from Sigma and Iduron (Manchester, UK), respectively. Structurally homogeneous heparin-derived oligosaccharides were synthesized using a chemoenzymatic approach. The purity analysis and structural characterization of the oligosaccharides were described previously (31, 32).

### Cell culture and isolation of human PBMCs and T cells

The IL-2-independent, IL-12-responsive human natural killer cell line, NK-92MI (ATCC; CRL-2408TM), was cultured in complete media consisting of  $\alpha$ -minimal essential medium supplemented with 12% FBS, 12% horse serum, 100 units/ml penicillin/streptomycin, 0.2 mM inositol, 0.02 mM folic acid, and 0.1 mM 2-mercaptoethanol. The mouse IL-12 responsive T cell line, 2D6, was cultured in RPMI 1640 medium supplemented with 10% FBS, 100 units/ml penicillin/streptomycin, 2 mM L-glutamine, and 250 pg/ml mIL-12. HEK-Blue<sup>TM</sup> IL-12

**Figure 5. Heparin-induced enhancement of IL-12 depends on sulfation level.** hIL-12 binding to heparin oligosaccharides was quantified via a novel microarray. The binding of Alexa Fluor 488-labeled hIL-12 (A) or mIL-12 (B) to the different heparin oligosaccharides was visualized and quantified via fluorescence microscopy. Six dodecasaccharides, including the high binding compounds 18 and 19, were selected for bioactivity studies (C and D). hIL-12 activity as measured by IFN- $\gamma$  production by NK-92MI cells (C) or secreted alkaline phosphatase by HEK-Blue<sup>TM</sup> IL-12 cells (D) was measured after co-culture with heparin compounds 18, 19, 21, 23–25 or LMWH (10  $\mu$ g/ml). Heparin compounds 18, 19, and LMWH significantly increased the bioactivity of hIL-12 in NK-92MI cells and HEK-Blue<sup>TM</sup> IL-12 cells ( $p < 0.0001$  versus hIL-12 alone via Tukey's post-test). Heparin compounds 21, 24, and 25 did not enhance the bioactivity of IL-12 in NK-92MI cells and HEK-Blue<sup>TM</sup> IL-12 cells ( $p > 0.05$  versus hIL-12 alone via Tukey's post-test). Heparin compound 23 did not enhance hIL-12 bioactivity in NK-92MI cells (\*\*\*,  $p < 0.0001$  versus IL-12 alone via Tukey's post-test) and modestly enhanced IL-12 bioactivity in HEK-Blue<sup>TM</sup> IL-12 cells ( $p < 0.0001$  versus IL-12 alone and  $p < 0.0001$  versus IL-12 plus LMWH via Tukey's post-test). Data bars in the bioactivity studies represent mean  $\pm$  S.D. of triplicate measurements. Experiments were performed in triplicate and repeated three times with similar results.

## Mechanisms of heparin-induced IL-12 modulation

cells (Invivogen, San Diego, CA) were maintained in Dulbecco's modified Eagle's medium supplemented with 2 mM L-glutamine, 10% FBS, 100 units/ml penicillin/streptomycin, and 100  $\mu\text{g}/\text{ml}$  normocin.

Human PBMCs were isolated from leukopaks on a density gradient (Lympholyte<sup>®</sup>-H; Cedarlane Labs). De-identified leukopaks from healthy donors were purchased from the New York Blood Center (New York, NY). Human T cells were isolated from PBMCs by negative selection with magnetic beads (Dynabeads<sup>®</sup> Untouched<sup>™</sup> human T cells kit; ThermoFisher Scientific). PBMCs and T cells were cultured in RPMI 1640 medium supplemented with 10% FBS, 1 mM sodium pyruvate, 2 mM L-glutamine, 10 mM HEPES, 100 units/ml penicillin/streptomycin. All experiments were performed in accordance with relevant guidelines and regulations at North Carolina State University.

### IL-12 bioactivity assay and cytokine measurement

IFN- $\gamma$  secretion from NK-92MI cells, PBMCs, and activated T cells was used as an indicator of hIL-12 bioactivity. T cells were activated by incubating  $10^6$  cells/ml with anti-CD3 and anti-CD28-coated super-paramagnetic beads (Dynabeads<sup>®</sup> human T-activator CD3/CD28; ThermoFisher Scientific) in cultured media at a bead/cell ratio of 1:1 for 3 days.

As described previously, cells were seeded in a 96-well plate at 20,000 cells/well (NK-92MI) or 500,000 cells/well (PBMCs and T cells) (17). hIL-12 was added to achieve final concentrations from 0 to 1000 pg/ml. Heparin was added to a final concentration ranging from 0 to 500  $\mu\text{g}/\text{ml}$ . Cells in hIL-12 alone or culture media alone served as controls. After 24 h, hIL-12-dependent secretion of IFN- $\gamma$  into the supernatant of the culture was quantified via enzyme-linked immunosorbent assay (ELISA) (88-7316-86; ThermoFisher Scientific). In other experiments, levels of human Th1/Th2/Th17 cytokines, including IL-2, IL-4, IL-6, IL-10, tumor necrosis factor- $\alpha$ , IFN- $\gamma$ , and IL-17A in culture supernatants were determined via BD Cytometric Bead Array kit (560484; BD Biosciences) and analyzed using FACSDiva<sup>™</sup> Software (BD Biosciences).

In the murine system, 2D6 cells were starved of mIL-12 overnight before culturing (20,000 cells/well) with increasing doses of heparin (0  $\mu\text{g}/\text{ml}$  to 500  $\mu\text{g}/\text{ml}$ ) and either mIL-12 (200 pg/ml) or hIL-12 (200 pg/ml) in a 96-well plate. After 24 h, IL-12-induced proliferation was examined via CellTiter-Glo<sup>®</sup> 3D cell viability assay (Promega, G9682).

HEK-Blue<sup>™</sup> IL-12 cells (Invivogen, San Diego) express a STAT4-inducible secreted embryonic alkaline phosphatase (SEAP) reporter gene that is triggered upon binding of IL-12 to IL-12R. HEK-Blue<sup>™</sup> IL-12 cells were seeded in a 96-well plate at 50,000 cells/well and cultured with 0–5 ng/ml hIL-12 and 0–500  $\mu\text{g}/\text{ml}$  heparin. After 24 h, SEAP concentrations in supernatants were developed with Quanta-Blue<sup>™</sup> (Invivogen, San Diego) and quantified via absorbance readings at 650 nm on a Citation microplate reader (Biotek, Winooski, VT).

### Intracellular flow cytometry

The following antibodies used for staining cell-surface markers were obtained from BD Biosciences: anti-human CD3 FITC (clone UCHT1), anti-human CD4 PerCP-Cit. (clone RPA-T4),

anti-human CD8 APC-R700 (clone RPA-T8), and anti-human CD56 PE-CF594 or PerCP-Cy5.5 (clone B159). Blocking of nonspecific Fc receptor was performed by incubating cells with 25  $\mu\text{g}/\text{ml}$  human Fc block (BD Biosciences) in staining buffer (PBS supplemented with 0.2% BSA and 0.09% sodium azide). For intracellular staining of IFN- $\gamma$ , protein transport inhibitor containing monensin (BD Biosciences) was added to the cells during induction. Cells were fixed in fixation/permeabilization solutions (BD Biosciences) using the manufacturer's recommended protocols. Anti-human IFN- $\gamma$  BV421 (clone B27) was used for intracellular IFN- $\gamma$  staining. Data were acquired using a BD FACSCelesta flow cytometer (BD Biosciences) and analyzed using FlowJo software (Tree Star, Ashland, OR). IFN- $\gamma^+$  cells were analyzed in the gated CD3<sup>+</sup> CD4<sup>+</sup> T cells, CD3<sup>+</sup> CD8<sup>+</sup> T cells, and CD3<sup>-</sup> CD56<sup>+</sup> NK cells as illustrated in the gating strategies (Figs. S1 and S2).

### Isothermal calorimetry

ITC experiments were performed on an iTC-200 (Malvern Inc.) at 25 °C. Both recombinant hIL-12 or mIL-12 (200  $\mu\text{M}$ ) and the heparin oligosaccharides (2 mM) were dissolved in 10 mM phosphate buffer (pH 7.2) containing 150 mM NaCl. The concentration of hIL-12 or mIL-12 to heparin oligosaccharides was maintained at a molar ratio of 1:10. All solutions were degassed prior to titration. Isothermal titrations were performed by injecting individual heparin oligosaccharides into hIL-12 or mIL-12 solutions in the reaction vessel. Isothermograms were obtained using 30 injections and were best-fit to a one-site/multiple-site binding model using the Origin<sup>™</sup> version 7.0 software supplied by Microcal. Necessary blank corrections were performed to eliminate contributions originating from heats of dilution. To account for inaccuracy associated with fitting of nonideal/nonsigmoidal binding isotherms, the  $K_d$  values are reported as  $K_d$  (apparent).

### Microarray of HS-derived compounds

A custom HS-microarray was fabricated as described previously (33). To prepare the array chip, HS oligosaccharides were dissolved in sodium phosphate buffer (pH 8.5, 50 mM) in concentrations of 50  $\mu\text{M}$ . The solution was spatially arrayed onto *N*-hydroxysuccinimide-activated slides (Nexterion<sup>®</sup> Slide H from SCHOTT, Jena, Germany) under ~50% relative humidity at 20 °C. The robotic arrayer S11 (from Scienion, Berlin, Germany) delivered 426 pl of the solution containing oligosaccharides to the array slide. The array spots had an average diameter of about 80  $\mu\text{m}$  with a distance of 400  $\mu\text{m}$  between the centers of adjacent spots. The slides were incubated overnight in a saturated  $(\text{NH}_4)_2\text{SO}_4$  chamber (81% relative humidity). The slides were then washed with water to remove the unreacted oligosaccharides from the surface. The remaining *N*-hydroxysuccinimidyl groups were blocked by placing slides in a solution that contained 50 mM ethanolamine in PBST (137 mM NaCl, 13.2 mM  $\text{Na}_2\text{HPO}_4$ , 1.56 mM  $\text{NaH}_2\text{PO}_4$ , 2.68 mM KCl, 0.01% Tween 20) at 50 °C for at least 1.5 h. Slides were rinsed several times with deionized water, and the residual liquid was dried by centrifugation.

The hybridization solution contained fluorescently IL-12 (10  $\mu\text{g}/\text{ml}$ ) and PBST (137 mM NaCl, 2.7 mM KCl, 4.3 mM



## Statistical analysis

Na<sub>2</sub>HPO<sub>4</sub>, 1.4 mM KH<sub>2</sub>PO<sub>4</sub>, 0.05% Tween 20), 20 mM Tris (pH 7.5), and 10% bovine serum albumin (BSA). The solution was placed between array slide and coverslip and incubated for 1 h at room temperature in a saturated (NH<sub>4</sub>)<sub>2</sub>SO<sub>4</sub> chamber (81% relative humidity). The slide was then washed with 45 ml of PBST solution containing BSA (1%) and Tris (20 mM) for 5 min in a clean 50-ml conical tube. The wash process was repeated twice before analyzing the slide with the array scanner as described below.

The array slides were scanned by a GenePix 4300 scanner (Molecular Dynamics). Scanning wavelength was 488 nm. Resolution was set at 10 μm. The array images were analyzed by GenePix Pro 7.2.29.002 software. Spots were automatically found, and spot deviations were manually fit to correct. Mean median fluorescence intensities of arrays were calculated by Array Quality Control software. Some thresholds were listed as follows: median signal-to-background, >10; mean of median background, <500; median signal-to-noise, >10; feature variation, 0.5; background variation, 0.5; features with saturated pixels, 0.1%; not found features, 7%; bad features, <7%.

## IL-12/IL-12R complex modeling

Molecular modeling was performed using PyMOL molecular visualization software (Schrodinger, LLC) in conjunction with ClusPro protein–protein docking software and the Phyre2 web portal (34–39). The intensive modeling mode of the Phyre2 web portal was used to predict the structure of each IL-12 receptor subunit ECD based on primary structure and homogeneity to known protein structures. Next, the human IL-12 protein (PDB code 1F45) was used as an input into the ClusPro software together with each receptor subunit individually to calculate their likely placement (35, 36). From the top clusters given by the software, files with correct subunit interactions, *i.e.* IL-12Rβ1 with p40 and IL-12Rβ2 with p35, and orientation were chosen (40, 41). These two criteria alone eliminated all but two models per receptor subunit for a total of four clusters. The final two clusters were eliminated based on the nonphysiological overlap of the receptor subunits when they were superimposed based on the hIL-12 protein in PyMOL.

Heparin-binding sites on each receptor subunit were predicted using ClusPro as well, using the heparin-docking function. The top-scoring segments for each of the subunits were selected and highlighted in the protein structure models. After each set of predictions was made, the location of each receptor in relation to the other was modeled by superimposing the IL-12 molecules onto each other using the “cealign” command of the alignment/superposition plugin in the PyMOL software. After the alignment of each individual interaction based on the IL-12 molecule, no further modifications to the model were performed.

Distances between heparin-binding sites within the hIL-12/hIL-12R complex were determined using PyMOL’s measurement tool. For each measurement, residues within the heparin-binding segments that were closest to each other were used as end points. Within these residues, the carbon atom was chosen to approximate the distance between heparin-binding sites.

Experiments were performed in triplicate and repeated three times with similar results. Two-tailed *t*-tests were used for comparisons of two groups such as positive percentages of intracellular IFN-γ in response to hIL-12 alone and hIL-12 plus heparin or binding affinities between heparin oligosaccharides and hIL-12 or mIL-12. Extra sum-of-squares *F* test was used to evaluate the difference of EC<sub>50</sub> value generated by hIL-12 alone and hIL-12 plus heparin. One-way ANOVA was used to discern differences in cytokine release from cells undergoing multiple treatments of a fixed concentration of hIL-12 and increasing concentrations of heparin. Two-way ANOVA was used to distinguish differences of cytokine release from cells undergoing combination treatments of hIL-12 and heparin. The Tukey post-test was used after the ANOVA to compare individual treatment groups. Statistical significance was accepted at the *p* ≤ 0.05 level. All analyses were conducted using GraphPad Prism 7 software (GraphPad Software).

**Author contributions**—K. G. N., F. B. G., R. K. G., S. K. T., and D. A. Z. conceptualization; K. G. N., F. B. G., J. L., S. K. T., and D. A. Z. data curation; K. G. N., S. J., and D. A. Z. formal analysis; K. G. N., J. J. H., S. J., R. K. G., G. S., J. B., B. K. F., J. L., S. K. T., and D. A. Z. investigation; K. G. N., F. B. G., J. J. H., S. J., R. K. G., G. S., J. B., and B. K. F. methodology; K. G. N., B. K. F., J. L., S. K. T., and D. A. Z. writing—original draft; K. G. N., F. B. G., J. J. H., R. K. G., J. B., G. R. P., R. J., B. K. F., J. L., S. K. T., and D. A. Z. writing—review and editing; F. B. G. visualization; J. B., G. R. P., R. J., B. K. F., J. L., S. K. T., and D. A. Z. resources; J. L., S. K. T., and D. A. Z. supervision; J. L., S. K. T., and D. A. Z. project administration; D. A. Z. funding acquisition.

**Acknowledgments**—We thank R. Doueiri and B. Chowdhury for technical assistance.

## References

- Hileman, R. E., Fromm, J. R., Weiler, J. M., and Linhardt, R. J. (1998) Glycosaminoglycan-protein interactions: definition of consensus sites in glycosaminoglycan binding proteins. *Bioessays* **20**, 156–167 [CrossRef Medline](#)
- Ornitz, D. M., Yayon, A., Flanagan, J. G., Svahn, C. M., Levi, E., and Leder, P. (1992) Heparin is required for cell-free binding of basic fibroblast growth factor to a soluble receptor and for mitogenesis in whole cells. *Mol. Cell. Biol.* **12**, 240–247 [CrossRef Medline](#)
- Loo, B. M., Kreuger, J., Jalkanen, M., Lindahl, U., and Salmivirta, M. (2001) Binding of heparin/heparan sulfate to fibroblast growth factor receptor 4. *J. Biol. Chem.* **276**, 16868–16876 [CrossRef Medline](#)
- Fannon, M., Forsten, K. E., and Nugent, M. A. (2000) Potentiation and inhibition of bFGF binding by heparin: a model for regulation of cellular response. *Biochemistry* **39**, 1434–1445 [CrossRef Medline](#)
- Najjam, S., Mulloy, B., Theze, J., Gordon, M., Gibbs, R., and Rider, C. C. (1998) Further characterization of the binding of human recombinant interleukin 2 to heparin and identification of putative binding sites. *Glycobiology* **8**, 509–516 [CrossRef Medline](#)
- Alvarez-Silva, M., and Borojevic, R. (1996) GM-CSF and IL-3 activities in schistosomal liver granulomas are controlled by stroma-associated heparan sulfate proteoglycans. *J. Leukocyte Biol.* **59**, 435–441 [CrossRef Medline](#)
- Clarke, D., Katoh, O., Gibbs, R. V., Griffiths, S. D., and Gordon, M. Y. (1995) Interaction of interleukin 7 (IL-7) with glycosaminoglycans and its biological relevance. *Cytokine* **7**, 325–330 [CrossRef Medline](#)
- Salek-Ardakani, S., Arrand, J. R., Shaw, D., and Mackett, M. (2000) Heparin and heparan sulfate bind interleukin-10 and modulate its activity. *Blood* **96**, 1879–1888 [Medline](#)



## Mechanisms of heparin-induced IL-12 modulation

- Gubler, U., Chua, A. O., Schoenhaut, D. S., Dwyer, C. M., McComas, W., Motyka, R., Nabavi, N., Wolitzky, A. G., Quinn, P. M., and Familletti, P. C. (1991) Coexpression of two distinct genes is required to generate secreted bioactive cytotoxic lymphocyte maturation factor. *Proc. Natl. Acad. Sci. U.S.A.* **88**, 4143–4147 [CrossRef Medline](#)
- Wolf, S. F., Temple, P. A., Kobayashi, M., Young, D., Dicig, M., Lowe, L., Dzialo, R., Fitz, L., Ferenz, C., and Hewick, R. M. (1991) Cloning of cDNA for natural killer cell stimulatory factor, a heterodimeric cytokine with multiple biologic effects on T and natural killer cells. *J. Immunol.* **146**, 3074–3081 [Medline](#)
- Schoenhaut, D. S., Chua, A. O., Wolitzky, A. G., Quinn, P. M., Dwyer, C. M., McComas, W., Familletti, P. C., Gately, M. K., and Gubler, U. (1992) Cloning and expression of murine IL-12. *J. Immunol.* **148**, 3433–3440 [Medline](#)
- Trinchieri, G. (2003) Interleukin-12 and the regulation of innate resistance and adaptive immunity. *Nat. Rev. Immunol.* **3**, 133–146 [CrossRef Medline](#)
- Jalah, R., Rosati, M., Ganneru, B., Pilkington, G. R., Valentin, A., Kulkarni, V., Bergamaschi, C., Chowdhury, B., Zhang, G.-M., Beach, R. K., Alicea, C., Broderick, K. E., Sardesai, N. Y., Pavlakis, G. N., and Felber, B. K. (2013) The p40 subunit of IL-12 promotes stabilization and export of the p35 subunit: implications for improved IL-12 cytokine production. *J. Biol. Chem.* **288**, 6763–6776 [CrossRef Medline](#)
- Hasan, M., Najjam, S., Gordon, M. Y., Gibbs, R. V., and Rider, C. C. (1999) IL-12 is a heparin-binding cytokine. *J. Immunol.* **162**, 1064–1070 [Medline](#)
- Jayanthi, S., Koppolu, Bp., Smith, S. G., Jalah, R., Bear, J., Rosati, M., Pavlakis, G. N., Felber, B. K., Zaharoff, D. A., and Kumar, T. K. (2014) Efficient production and purification of recombinant human interleukin-12 (IL-12) overexpressed in mammalian cells without affinity tag. *Protein Expr. Purif.* **102**, 76–84 [CrossRef Medline](#)
- Garnier, P., Mummery, R., Forster, M. J., Mulloy, B., Gibbs, R. V., and Rider, C. C. (2018) The localisation of the heparin binding sites of human and murine interleukin-12 within the carboxyl-terminal domain of the P40 subunit. *Cytokine* **110**, 159–168 [CrossRef Medline](#)
- Jayanthi, S., Koppolu, B. P., Nguyen, K. G., Smith, S. G., Felber, B. K., Kumar, T. K. S., and Zaharoff, D. A. (2017) Modulation of interleukin-12 activity in the presence of heparin. *Sci. Rep.* **7**, 5360 [CrossRef Medline](#)
- Leonard, J. P., Sherman, M. L., Fisher, G. L., Buchanan, L. J., Larsen, G., Atkins, M. B., Sosman, J. A., Dutcher, J. P., Vogelzang, N. J., and Ryan, J. L. (1997) Effects of single-dose interleukin-12 exposure on interleukin-12-associated toxicity and interferon- $\gamma$  production. *Blood* **90**, 2541–2548 [Medline](#)
- Soares da Costa, D., Reis, R. L., and Pashkuleva, I. (2017) Sulfation of glycosaminoglycans and its implications in human health and disorders. *Annu. Rev. Biomed. Eng.* **19**, 1–26 [CrossRef Medline](#)
- Xu, X., Takano, R., Nagai, Y., Yanagida, T., Kamei, K., Kato, H., Kamikubo, Y., Nakahara, Y., Kumeda, K., and Hara, S. (2002) Effect of heparin chain length on the interaction with tissue factor pathway inhibitor (TFPI). *Int. J. Biol. Macromol.* **30**, 151–160 [CrossRef Medline](#)
- Rezaie, A. R. (2007) Heparin chain-length dependence of factor Xa inhibition by antithrombin in plasma. *Thromb. Res.* **119**, 481–488 [CrossRef Medline](#)
- Hochart, H., Jenkins, P. V., Preston, R. J., Smith, O. P., White, B., and O'Donnell, J. (2008) Concentration-dependent roles for heparin in modifying lipopolysaccharide-induced activation of mononuclear cells in whole blood. *Thromb. Haemost.* **99**, 570–575 [CrossRef Medline](#)
- Mehrotra, P. T., Donnelly, R. P., Wong, S., Kanegane, H., Geremew, A., Mostowski, H. S., Furuke, K., Siegel, J. P., and Bloom, E. T. (1998) Production of IL-10 by human natural killer cells stimulated with IL-2 and/or IL-12. *J. Immunol.* **160**, 2637–2644 [Medline](#)
- Tam, Y. K., Maki, G., Miyagawa, B., Hennemann, B., Tonn, T., and Klingemann, H. G. (1999) Characterization of genetically altered, interleukin 2-independent natural killer cell lines suitable for adoptive cellular immunotherapy. *Hum. Gene Ther.* **10**, 1359–1373 [CrossRef Medline](#)
- Choijsiluren, G., Jhou, R. S., Chou, S. F., Chang, C. J., Yang, H. I., Chen, Y. Y., Chuang, W. L., Yu, M. L., and Shih, C. (2017) Heparin at physiological concentration can enhance PEG-free *in vitro* infection with human hepatitis B virus. *Sci. Rep.* **7**, 14461 [CrossRef Medline](#)
- Scott, J. E., Bosworth, T. R., Cribb, A. M., and Gressner, A. M. (1994) The chemical morphology of extracellular matrix in experimental rat liver fibrosis resembles that of normal developing connective tissue. *Virchows Arch.* **424**, 89–98 [Medline](#)
- McKee, R. F., Hodson, S., Dawes, J., Garden, O. J., and Carter, D. C. (1992) Plasma concentrations of endogenous heparinoids in portal hypertension. *Gut* **33**, 1549–1552 [CrossRef Medline](#)
- Casanova, J. L., and Abel, L. (2002) Genetic dissection of immunity to mycobacteria: the human model. *Annu. Rev. Immunol.* **20**, 581–620 [CrossRef Medline](#)
- Fieschi, C., Bosticardo, M., de Beaucoudrey, L., Boisson-Dupuis, S., Feinberg, J., Santos, O. F., Bustamante, J., Levy, J., Candotti, F., and Casanova, J. L. (2004) A novel form of complete IL-12/IL-23 receptor  $\beta$ 1 deficiency with cell surface-expressed nonfunctional receptors. *Blood* **104**, 2095–2101 [CrossRef Medline](#)
- Vignali, D. A., and Kuchroo, V. K. (2012) IL-12 family cytokines: immunological playmakers. *Nat. Immunol.* **13**, 722–728 [CrossRef Medline](#)
- Xu, Y., Cai, C., Chandarajoti, K., Hsieh, P. H., Li, L., Pham, T. Q., Sparkenbaugh, E. M., Sheng, J., Key, N. S., Pawlinski, R., Harris, E. N., Linhardt, R. J., and Liu, J. (2014) Homogeneous low-molecular-weight heparins with reversible anticoagulant activity. *Nat. Chem. Biol.* **10**, 248–250 [CrossRef Medline](#)
- Xu, Y., Chandarajoti, K., Zhang, X., Pagadala, V., Dou, W., Hoppensteadt, D. M., Sparkenbaugh, E. M., Cooley, B., Daily, S., Key, N. S., Severynse-Stevens, D., Fareed, J., Linhardt, R. J., Pawlinski, R., and Liu, J. (2017) Synthetic oligosaccharides can replace animal-sourced low-molecular weight heparins. *Sci. Transl. Med.* **9**, ean5954 [CrossRef Medline](#)
- Yang, J., Hsieh, P. H., Liu, X., Zhou, W., Zhang, X., Zhao, J., Xu, Y., Zhang, F., Linhardt, R. J., and Liu, J. (2017) Construction and characterisation of a heparan sulphate heptasaccharide microarray. *Chem. Commun.* **53**, 1743–1746 [CrossRef](#)
- Comeau, S. R., Gatchell, D. W., Vajda, S., and Camacho, C. J. (2004) ClusPro: an automated docking and discrimination method for the prediction of protein complexes. *Bioinformatics* **20**, 45–50 [CrossRef Medline](#)
- Comeau, S. R., Gatchell, D. W., Vajda, S., and Camacho, C. J. (2004) ClusPro: a fully automated algorithm for protein–protein docking. *Nucleic Acids Res.* **32**, W96–W99 [CrossRef Medline](#)
- Kozakov, D., Brenke, R., Comeau, S. R., and Vajda, S. (2006) PIPER: an FFT-based protein docking program with pairwise potentials. *Proteins* **65**, 392–406 [CrossRef Medline](#)
- Kozakov, D., Hall, D. R., Xia, B., Porter, K. A., Padhorny, D., Yueh, C., Beglov, D., and Vajda, S. (2017) The ClusPro web server for protein–protein docking. *Nat. Protoc.* **12**, 255–278 [CrossRef Medline](#)
- Schrödinger, L. (2010) *The PyMOL Molecular Graphics System*, Version 1.r1, Schrödinger, LLC, New York
- Kelley, L. A., Mezulis, S., Yates, C. M., Wass, M. N., and Sternberg, M. J. (2015) The Phyre2 web portal for protein modeling, prediction and analysis. *Nat. Protoc.* **10**, 845–858 [CrossRef Medline](#)
- Chua, A. O., Chizzonite, R., Desai, B. B., Truitt, T. P., Nunes, P., Minetti, L. J., Warrior, R. R., Presky, D. H., Levine, J. F., and Gately, M. K. (1994) Expression cloning of a human IL-12 receptor component. A new member of the cytokine receptor superfamily with strong homology to gp130. *J. Immunol.* **153**, 128–136 [Medline](#)
- Presky, D. H., Yang, H., Minetti, L. J., Chua, A. O., Nabavi, N., Wu, C.-Y., Gately, M. K., and Gubler, U. (1996) A functional interleukin 12 receptor complex is composed of two  $\beta$ -type cytokine receptor subunits. *Proc. Natl. Acad. Sci. U.S.A.* **93**, 14002–14007 [CrossRef Medline](#)